Journal of the European Ceramic Society **18** (1998) 1063–1071

PII: S0955-2219(97)00215-X
0955-2219/98/$19.00 + 0.00

Grain Boundary Mobility of $BaTiO_3$ Doped with Aliovalent Cations

M. N. Rahaman* and R. Manalert

University of Missouri-Rolla, Department of Ceramic Engineering, Rolla, Missouri 65401, USA

(Received 31 January 1997; accepted 20 November 1997)

Abstract

The effect of three aliovalent cations, Nb^{5+}, La^{3+} and Co^{2+}, on the grain growth kinetics of nearly fully dense $BaTiO_3$ (Ba/Ti atomic ratio = 1·001) was measured in O_2 at 1300°C and for dopant concentrations of up to 1·25 atomic per cent (at%). For the donor cation Nb^{5+}, the boundary mobility initially increased with cation concentration but then decreased markedly above a doping threshold of 0·3–0·5 at%. The boundary mobility of the $BaTiO_3$ doped with the acceptor cation Co^{2+} decreased monotonically with dopant concentration. At a cation concentration of 0·75 at%, the boundary mobility was reduced by a factor of approximately 25, 10 and 50 times by Nb^{5+}, La^{3+} and Co^{2+}, respectively. A major role of the dopants is seen to be their ability to influence the boundary mobility. The effects of the dopants on the boundary mobility are discussed in terms of the defect chemistry and the space-charge concept. © *1998 Published by Elsevier Science Limited. All rights reserved*

1 Introduction

Following the work of Coble[1] on MgO-doped Al_2O_3, the use of dopants has been shown to be a very effective approach for the production, by conventional sintering, of ceramics with high density and fine grain size such as are normally required for most advanced technological applications.[2] However, the role of the dopant has been the subject of considerable debate. While progress has been made in a few recognized examples,[3–9] e.g. Al_2O_3, $BaTiO_3$, ZrO_2 and CeO_2, a considerable gap exists in the understanding of the dopant role.

A major reason for this gap is the multiplicity of functions that a dopant can display.[2–4] Faced with the problem of the multiplicity of dopant roles, Brook[10] suggested a combined approach for achieving progress. The approach consists, on one hand, of survey studies to provide valid generalization and on the other of detailed investigations of individual systems to obtain a full picture of a particular interaction. The work of Harmer and coworkers[3,11] on the MgO-doped Al_2O_3 system provides an important example of detailed studies to characterize a given system. The results indicate that while the MgO affects the lattice and surface diffusion coefficients, the single most important effect is its ability to reduce significantly the grain boundary mobility. Survey studies by Hwang and Chen[6] of the influence of aliovalent dopants on grain growth in tetragonal zirconia polycrystals (TZP) have reported the importance of additive cation charge on segregation and of additive cation size on the boundary mobility. For CeO_2 doped with divalent and trivalent cations,[7–9] survey studies have shown the importance of the additive concentration, cation size and cation charge for controlling the grain growth.[9] Detailed studies[8] have indicated that at lower dopant concentration (intrinsic regime), the gain boundary mobility is controlled by the grain boundary diffusion of the host cations. At higher concentration (extrinsic regime), the mobility is controlled by solute drag through the lattice.

Barium titanate, $BaTiO_3$, is an important ferroelectric material which has been studied extensively for nearly 50 years. Generally,[12,13] optimization of the ferroelectric behavior of $BaTiO_3$ requires a high density and controlled, homogeneous microstructure with grain size of $\approx 1\ \mu m$. Since the use of dopants forms a very effective approach for microstructural control,[14] considerable work has been performed in an attempt to characterize the defect structure of $BaTiO_3$ and its effect on sintering and grain growth behavior. Previous research has provided information on the defect structure[15–20] and the grain boundary chemistry[21] of $BaTiO_3$. This background suggests that $BaTiO_3$ would be

*To whom correspondence should be addressed.

an excellent model system for investigating the influence of aliovalent dopants on sintering.

Donor cations, i.e. ions of higher valence than the host cation (e.g. La^{3+} for Ba^{2+} and Nb^{5+} for Ti^{4+}) at a concentration of a few tenths of 1 at% lead to a dramatic change in the behavior of $BaTiO_3$. This phenomenon is sometimes referred to as the 'doping anomaly' or 'grain size anomaly'. Below this doping threshold, the conductivity increases with the donor concentration and the $BaTiO_3$ is semi-conducting. The sintered material also has a coarse- grained microstructure. Increasing the donor concentration above the threshold, however, results in a rapid decrease in the conductivity (the material becomes insulating) and the production of a fine-grained microstructure. The phenomenon is essentially independent of the elemental composition of the donor, thereby indicating that the change in electrical behavior is directly related to the change in microstructure.

While all donor dopants (at a concentration above the threshold) are effective in inhibiting grain growth, acceptor dopants (i.e. ions of a valence lower than that of the host cation) produce mixed behavior,[4] i.e. some acceptors (e.g. Co^{2+}) inhibit grain growth while others (e.g. Cu) enhance grain growth. The origins of the mixed behavior caused by the use of acceptor dopants are unclear. However, it has been found[4] that if a donor (e.g. Ta^{5+}) and an acceptor that inhibits grain growth (e.g. Co^{2+}) are present in compensating concentrations (i.e. the sum of the effective charges is equal to zero), then grain growth is not inhibited. This indicates that defect charge compensation may have a significant effect on grain growth.

The sintering of $BaTiO_3$ is also dependent on the stoichiometry of the compound. The solubility of TiO_2 and of BaO in $BaTiO_3$ is very limited,[22] i.e. less than $\approx$ 100 ppm. For $BaTiO_3$ materials with a small excess of TiO_2 (i.e. Ba/Ti atomic ratio less than 0·999), the excess TiO_2 reacts with $BaTiO_3$ to form a second phase, $Ba_6Ti_{17}O_{40}$, which has a eutectic with $BaTiO_3$ at $\approx$ 1320°C. The liquid phase which forms above the eutectic temperature is beneficial for densification but can also enhance grain growth. An excess of BaO (i.e. Ba/Ti atomic ratio greater than 1·001) leads to the formation of a second phase, Ba_2TiO_4, and to a reduction in the densification and grain growth rates.[23]

It is clear that dopants have a profound effect on the microstructural evolution of $BaTiO_3$. However, in addition to the variety of functions that a dopant can display, an understanding of the dopant role is further complicated by the presence of impurities, the effect of the Ba/Ti atomic ratio and the formation of a second phase, particularly a liquid phase above the eutectic temperature for Ba/Ti less than 0·999.

In the present work, the effect of three aliovalent cations, Nb^{5+}, La^{3+} and Co^{2+}, on the grain growth kinetics of nearly fully dense $BaTiO_3$, prepared from a high-purity, fine-grained powder (Ba/Ti atomic ratio = 1·001), was measured in O_2 at 1300°C and for dopant concentrations of up to 1·25 at%. An important feature of the work is the ability to obtain samples with nearly full density at a sintering temperature below that of the eutectic (1563°C) in the $BaTiO_3/Ba_2TiO_4$ system as well as that (1320°C) in the excess TiO_2 side. In this way, the effects associated with impurities and the presence of a liquid phase are significantly reduced.

2 Experimental Procedure

The dense samples used for the grain growth studies were prepared by sintering powder compacts at 1300°C. The $BaTiO_3$ powder was provided by Sakai Chemical Industry Co., Japan. The characteristics of the powder (Lot BT-01) as described by the manufacturer are given in Table 1. In the present work, the powder was further characterized by X-ray diffraction (Scintag XDS 2000) and by transmission electron microscopy (TEM). In the TEM analysis, samples were prepared by dispersing the powder in ethanol and then putting a drop of the suspension on a perforated carbon film and allowing it to dry. The microstructure of the powders was observed in a Philips EM-420 transmission electron microscope (TEM). A micrograph of the powder is given in Fig. 1.

Niobium chloride, lanthanum nitrate and cobalt nitrate were used to achieve the required doping at cation concentrations ranging from 0·25 to 1·25 at%. (The niobium and lanthanum salts, purity 99·999% and 99·99%, respectively, were obtained from AESAR/Johnson Matthey, Ward Hill, MA, USA and the cobalt nitrate, purity

Table 1. Characteristics of the fine-grained $BaTiO_3$ powder used in the present work. (Lot BT-01. Data from the manufacturer, Sakai Chemical Industry Co., Japan)

Characteristic	*Value*	*Testing method/conditions*
Average particle size	0·1 μm	SEM
Specific surface area	13·5 $m^2 g^{-1}$	BET method
Moisture content	0·4 wt%	at 105°C
Ignition loss	1·55 wt%	at 1200°C
Ba/Ti atomic ratio	1·001	XRF
SrO	0·01 wt%	ICP
CaO	< 0·001 wt%	ICP
Na_2O	0·002 wt%	ICP
SiO_2	0·003 wt%	ICP
Al_2O_3	< 0·001 wt%	ICP
Fe_2O_3	0·001 wt%	ICP

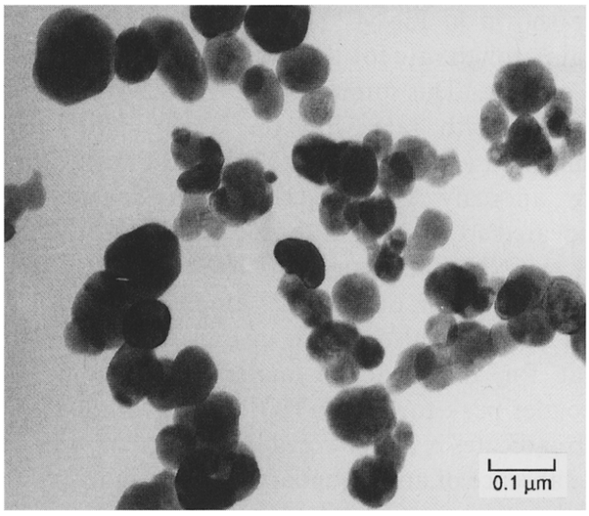

Fig. 1. TEM of the as-received $BaTiO_3$ powder.

99·999% was obtained from Aldrich Chemical Co., Milwaukee, WI, USA.) The procedure described by Kahn[24] was used for doping the $BaTiO_3$ powder with Nb^{5+}. In the process, the niobium chloride was first reacted with ethylene glycol. The precipitated material was repeatedly washed with water and redissolved in ethylene glycol to remove the chlorine ions. The precipitate was then hydrolyzed and admixed by stirring a 1:1 solution (by volume) of water and ethylene glycol with the $BaTiO_3$ powder. The resultant slurry was dried at 150°C. For doping with the other cations, the nitrate was dissolved in anhydrous ethanol and the $BaTiO_3$ powder was added to the solution and mixed thoroughly by stirring. The mixture was dried, under vigorous stirring, to ensure homogeneity of the additive. All processing was carried out using Teflon labware in a dust-free environment, and the procedure was kept as consistent as possible from additive to additive. The doped powders were calcined in air for 2 h at 900°C in a Pt crucible and then ground in a plastic mortar and pestle. For comparison, the same procedure was used for the undoped $BaTiO_3$ powder but without the addition of the dopant.

Compacts (6 mm in diameter by 6 mm) were formed by uniaxial pressing of the powder in a tungsten carbide die ($\approx$ 20 MPa), the contact surfaces of which were coated with stearic acid. The green densities of the samples were within a narrow range of $\approx$ 0·48–0·52 of the theoretical density of $BaTiO_3$ (assumed to be 6·02 g cm^{-3}).

The powder compacts were sintered in O_2 in a dilatometer (1600°C; Theta Industries, Port Washington, NY, USA) that allowed continuous monitoring of the shrinkage kinetics. The sample holder, push rods and protection tube of the dilatometer were made from high purity Al_2O_3 and the compacts were separated from the contact surfaces of the Al_2O_3 by Pt foil. The samples were heated at a constant rate of 5°C min^{-1} to 1300°C and held at this temperature for times ranging from 0 to 24 h after which they were cooled (at ~25°C min^{-1}). The final densities were determined from the initial density of the sample and the measured shrinkage and the values were checked using the Archimedes method.

The microstructure of the sintered materials was observed by scanning electron microscopy, SEM (JEOL-2000FXII), of fractured surfaces or of polished and thermally etched surfaces. Thermal etching was conducted for 2 h at 1200°C. The average grain size was determined by the linear intercept method[25,26] from $\approx$ 150 grains for each sample. In addition, for dense samples of undoped and Nb-doped $BaTiO_3$ (relative density greater than 0·98), the average grain size and the distribution in sizes were determined from micrographs of thermally etched, polished surfaces by computerized image analysis (NIH Image software). For each grain, the intercept length was taken as the diameter of the circle with an area equal to the computed value. At least 150 grains were analyzed for each sample.

3 Results

The density data and the microstructural observations indicated that the compacts reached densities greater than 98% of the theoretical value after 1 to 2 h at 1300°C for undoped and Nb-doped $BaTiO_3$ and after 3 to 4 h at the same temperature for Co-doped and La-doped $BaTiO_3$. As outlined later, the initial time for grain growth was taken as the time when the density of the sample was greater than 98% of the theoretical, thereby reducing significantly the effects of pores on the grain growth kinetics.

Figure 2 shows scanning electron micrographs of undoped $BaTiO_3$ held for 1, 8 and 16 h at 1300°C. Some residual porosity is evident after 1 h but it disappeared at longer heating times. Furthermore, no evidence was found for the growth of abnormally large grains. In order to further ascertain whether abnormal grain growth had occurred, the grain size distribution of the undoped $BaTiO_3$ heated for 4 h at 1300°C was analyzed. The results are plotted in Fig. 3 as the relative frequency of grains in a given size interval (normalized to a maximum value of 1) versus the reduced grain size (actual size divided by the average size). The majority of the grains have a size centered on the average and the absence of a secondary peak at larger sizes is a further indication of the absence of abnormal grain growth.

Microstructures of $BaTiO_3$ doped with 0·25 and 0·75 at% Nb and held for 1, 4 and 8 h at 1300°C

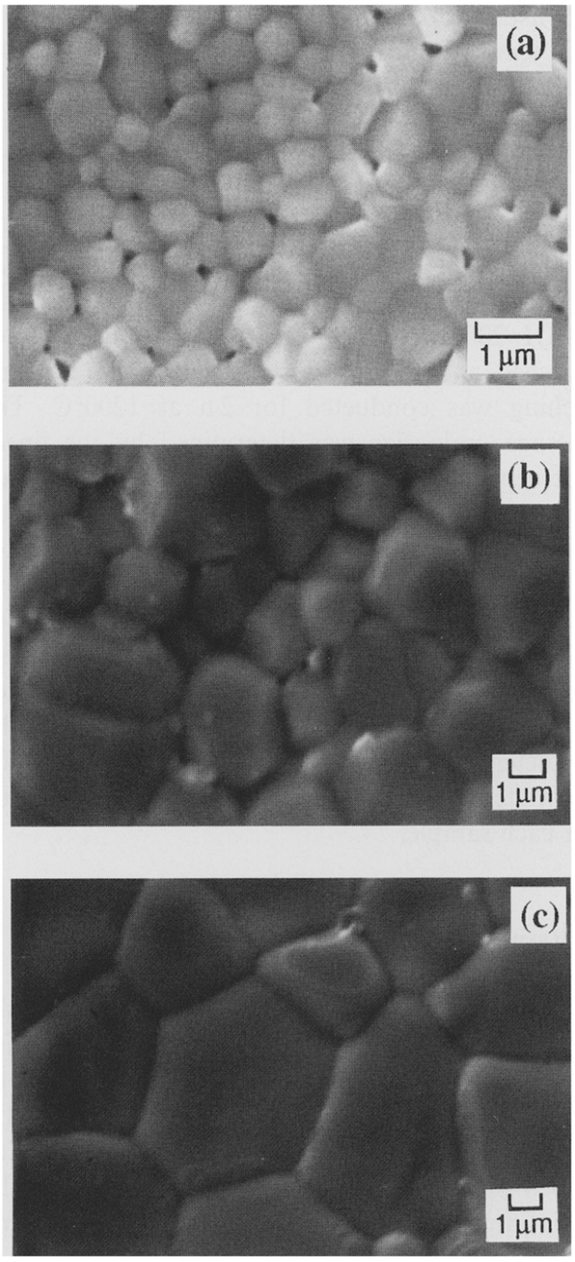

Fig. 2. SEM showing grain growth in undoped $BaTiO_3$ during heating at 1300°C for (a) 1 h, (b) 8 h and (c) 16 h.

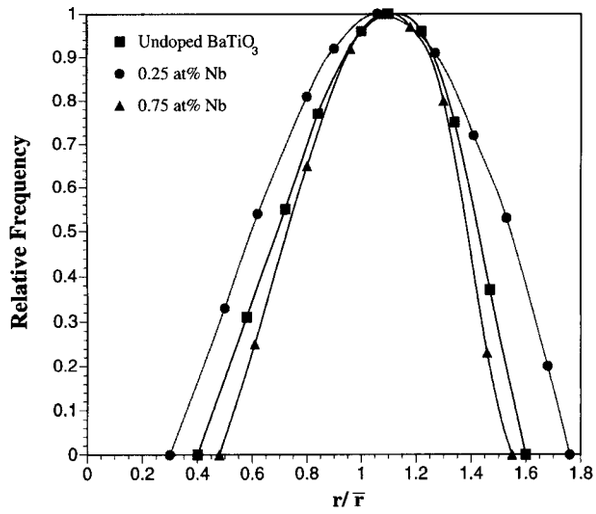

Fig. 3. Grain size distribution plotted as a function of the reduced grain size (actual grain size divided by the average size) for undoped $BaTiO_3$ and Nb-doped $BaTiO_3$ heated for 4 h at 1300°C.

are shown in Fig. 4. The significant difference in grain growth rate for the two Nb^{5+} concentrations is evident. This pronounced change-over in the grain growth rate with the donor cation concentration ($\approx$ 0·3 to 0·5 at%) is the so-called doping anomaly in $BaTiO_3$. Grain growth also appeared to be normal during heating (up to 16 h for the Nb-doped samples). The normalized grain size distribution data of the samples heated for 4 h at 1300°C are also shown in Fig. 3. Compared to that for the undoped material, the somewhat broader peak for the $BaTiO_3$ doped with 0·25 at% Nb indicates a larger spread in the grain sizes but the absence of any secondary peaks is an indication of the absence of abnormal grain growth.

The grain boundary mobility, M_b, can be estimated from the grain growth kinetics by the equation:[14]

$$\frac{dG}{dt} = \frac{M_b \gamma_b}{G} \tag{1}$$

where G is the grain size, γ_b is the specific energy of the grain boundary and t is the time. Assuming that M_b and γ_b are independent of time, then integration of eqn (1) leads to the parabolic grain growth law:

$$G^2 - G_o^2 = 2M_b\gamma_b(t - t_o) \tag{2}$$

where G_o is the grain size at an initial time t_o. In practice, it is common to find grain growth exponents varying from 2 to 4. This variation can be interpreted simply as being due to a decreasing M_b. According to eqn (2), a plot of $G^2 - G_o^2$ versus $t - t_o$ yields a curve with a slope equal to $2M_b\gamma_b$. In the present work, a straight line passing through the origin was fitted to the data to provide the average value of $2M_b\gamma_b$ for the duration of the grain growth experiment. Furthermore, to avoid any significant influence of porosity on the grain boundary mobility, the time t_o at 1300°C was chosen so that the sintered density of the samples was at least 98% of the theoretical value.

Figure 5 shows that the grain growth data for the undoped $BaTiO_3$ and for the $BaTiO_3$ doped with up to 1·25 at% Nb^{5+}. The average grain sizes for the undoped material and the material doped with 0·25 at% Nb were measured from polished and thermally etched surfaces. For the fine-grained material containing 0·75 and 1·25 at% Nb, the average grain sizes were measured from micrographs of the fractured surfaces. For the $BaTiO_3$ doped with 0·75 at% and heated for 16 h at 1300°C, the average grain size determined from

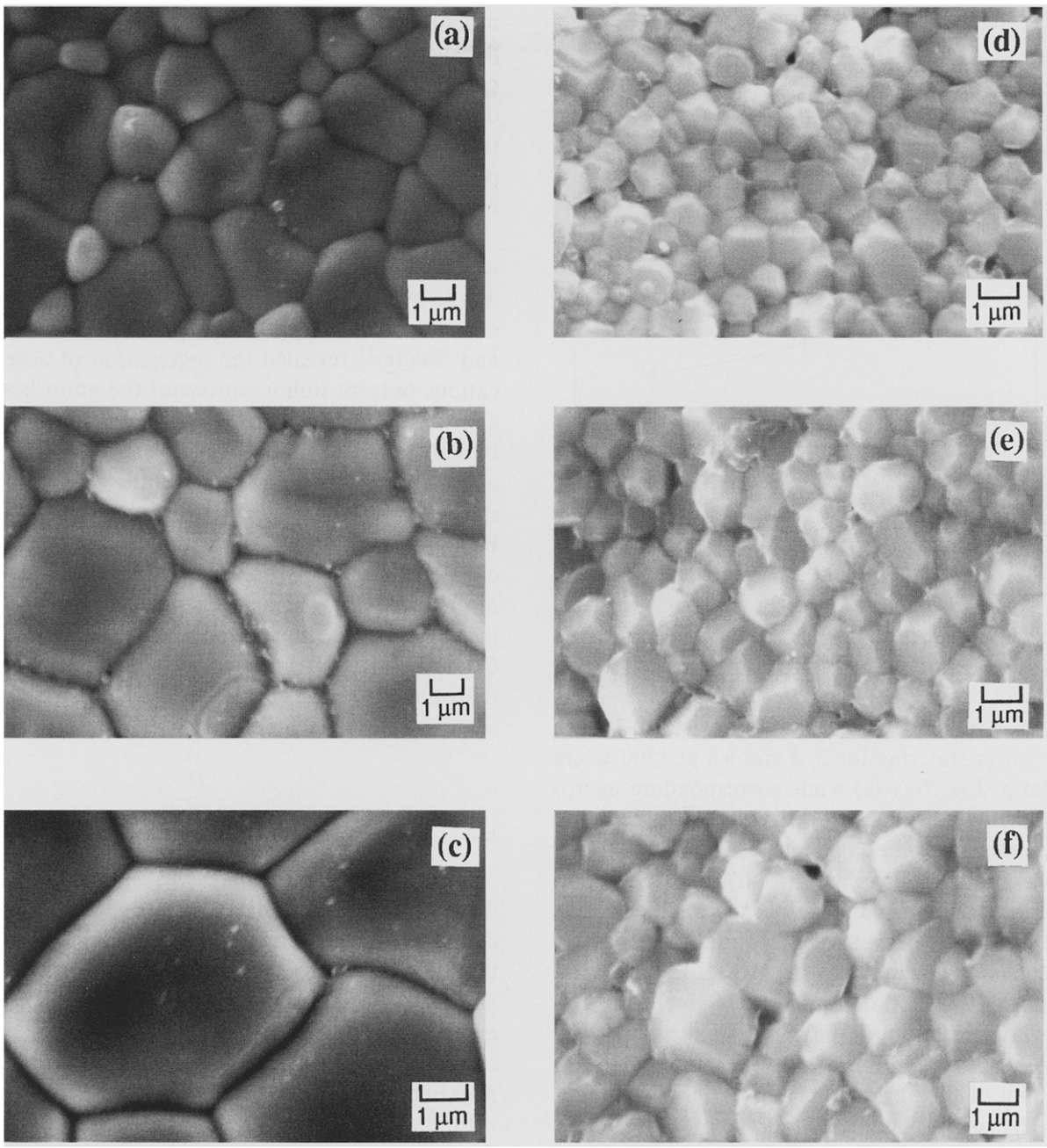

Fig. 4. SEM of the polished and thermally etched surfaces of $BaTiO_3$ doped with 0·25 at% Nb^{5+} [(a)–(c)] and the fractured surfaces of $BaTiO_3$ doped with 0·75 at% Nb^{5+} [(d)–(f)]. The samples were heated at 1300°C for: (a), (d) 1 h; (b), (e) 4 h and (c), (f) 8 h.

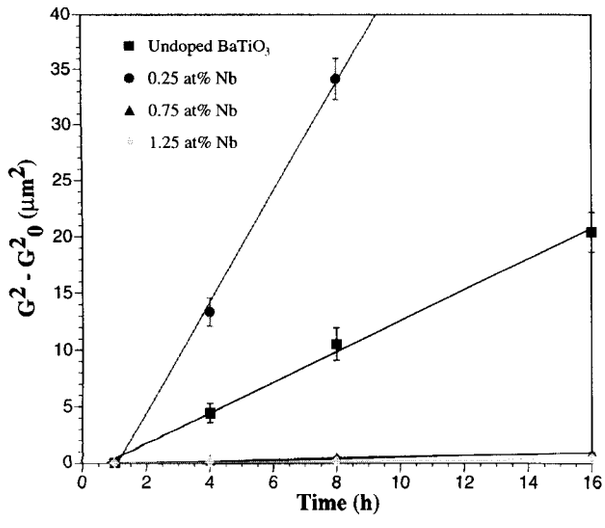

Fig. 5. Grain growth kinetics at 1300°C for undoped $BaTiO_3$ and Nb-doped $BaTiO_3$.

polished and thermally etched surfaces differed by $< 10\%$ from the value determined from fractured surfaces, indicating that the error introduced by using the data determined from the fractured surfaces was not significant. Assuming that γ_b is approximately constant, the normalized boundary mobility, M'_b, taken as the boundary mobility of the doped $BaTiO_3$ relative to that for the undoped $BaTiO_3$, is plotted in Fig. 6 as a function of the Nb^{5+} concentration. The value of M'_b increases initially with Nb^{5+} concentration, reaching a value of ≈ 4 at 0·25 at% but then decreases dramatically with increasing Nb^{5+} concentration to a value of 0·04 at 0·75 at%, i.e. for a change in Nb^{5+} concentration from 0·25 to 0·75 at%, M'_b decreases by a factor of ≈ 100. A further increase in the Nb^{5+}

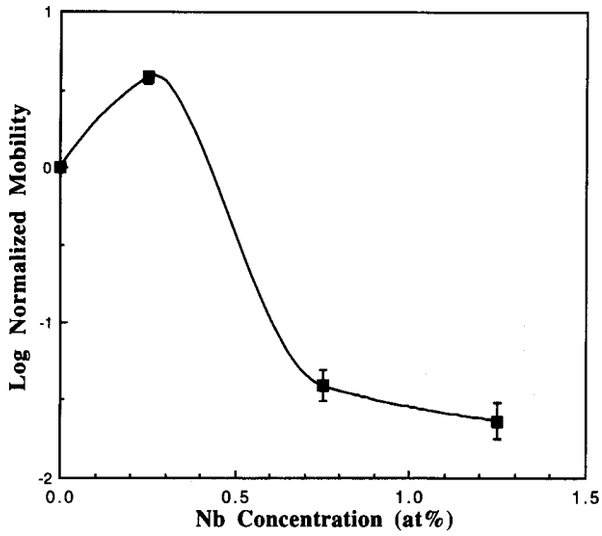

Fig. 6. Grain boundary mobility of Nb-doped $BaTiO_3$, normalized to that of undoped $BaTiO_3$, as a function of Nb^{5+} concentration.

concentration to 1·25 at% produces only a small reduction in M'_b compared to the value at 0·75 at%.

Microstructures of $BaTiO_3$ doped with 0·75 at% Co^{2+} after sintering for 2, 4 and 8 h at 1300°C are shown in Fig. 7(a)–(c) while corresponding microstructures for $BaTiO_3$ doped with 0·75 at% La^{3+} after sintering at the same temperature for 4, 8 and 16 h are shown in Fig. 7(d)–(f). Grain growth appears to be normal. Furthermore, plots of the grain size distribution for the Co-doped and La-doped samples sintered for 4 h at 1300°C were found to have approximately the same shapes as those for the undoped $BaTiO_3$ and the Nb-doped samples shown in Fig. 3.

A plot of the normalized grain boundary mobility, M'_b, as a function of Co^{2+} concentration is shown in Fig. 8. Compared to the Nb-doped $BaTiO_3$, the value of M'_b decreases monotonically with the Co^{2+} concentration, i.e. Co^{2+} inhibits grain growth for all of the concentrations investigated and there is no doping threshold.

Figure 9 shows the grain growth kinetics for undoped $BaTiO_3$ and $BaTiO_3$ doped separately with 0·75 at% of Nb^{5+}, Co^{2+} and La^{3+}. While all three cations are very effective for the inhibition of grain growth, Nb^{5+} and Co^{2+} are more effective than La^{3+}. At this dopant concentration, the boundary mobility of $BaTiO_3$ is reduced by a factor of approximately 50, 25 and 10 for Co^{2+}, Nb^{5+} and La^{3+}, respectively.

4 Discussion

The results indicate that a major role of the dopants is their ability to influence the boundary mobility. Furthermore, the difference in the dependence of the boundary mobility on the cation concentration (Figs 6 and 8) indicates that the dopant role for the donor Nb^{5+} is different from that for the acceptor Co^{2+}. Some observations pertinent to the understanding of the dopant role may be made at this stage.

As mentioned earlier, the grain boundary chemistry of $BaTiO_3$ has been investigated in earlier work. An analysis using scanning transmission electron microscopy (STEM) performed by Chiang and Takagi[21] revealed the segregation of acceptor cations but not donor cations at the grain boundaries in $BaTiO_3$ and $SrTiO_3$. According to the grain boundary model proposed by Chiang and Takagi, accumulation of the acceptor solute in the negative space charge is expected in the case of Co-doped $BaTiO_3$. Assuming that the segregated cations control the boundary mobility, then the solute drag mechanism proposed by Cahn[27] may provide an interpretation of the reduction in M_b (Fig. 8) in Co-doped $BaTiO_3$. According to the Cahn model, the boundary mobility is given approximately by an equation of the form:

$$M_b = \frac{D}{\Delta C k T} \tag{3}$$

where D is the diffusivity of the dopant cation, ΔC is the excess concentration of the dopant cation in the grain boundary, k is the Boltzmann constant and T is the absolute temperature. It may be expected that ΔC will increase with the Co^{2+} concentration, leading to a monotonically decreasing M_b (Fig. 8).

In the case of donor dopants, Fig. 6 shows a dramatic variation in M_b with Nb^{5+} concentration. As outlined earlier, the occurrence of the doping threshold is an indication that donor cations influence M_b by a solid solution mechanism. Furthermore, the absence of measurable segregation of donor cations[21] at the $BaTiO_3$ grain boundaries can be taken to rule out a solute drag mechanism by the donor cations. Below the doping threshold, a possible defect reaction for the incorporation of Nb^{5+} into $BaTiO_3$ can be written in the Kroger-Vink notation as:[19]

$$4BaO + Nb_2O_5 \Rightarrow 4Ba_{Ba}^{X} + 4Nb_{Ti}^{\cdot} + 12O_O^{X} + O_2 + 4e' \tag{4}$$

Above the doping threshold, assuming that ionic compensation occurs by the formation of Ti vacancies,[15] a possible defect reaction is:

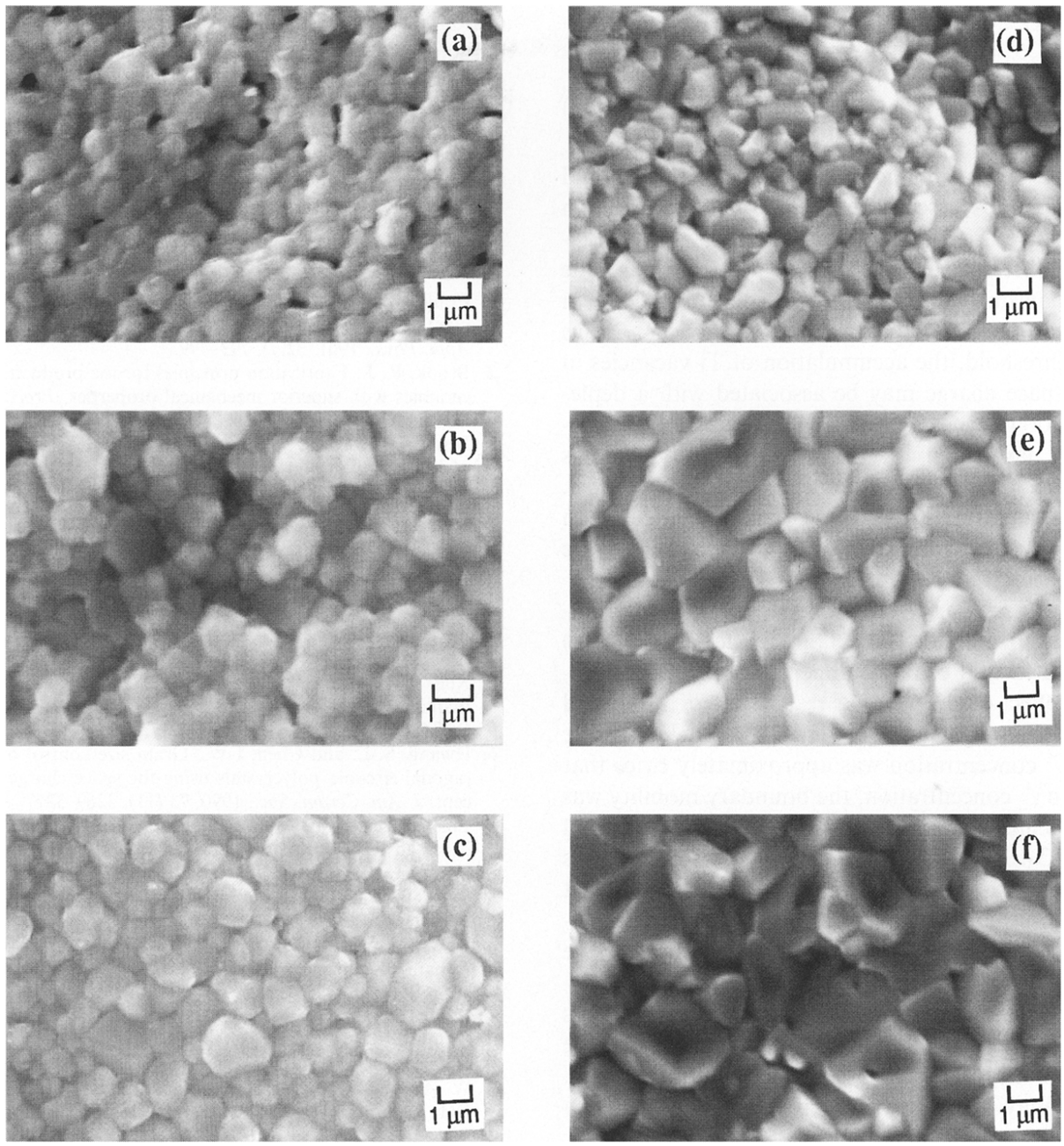

Fig. 7. SEM of the fractured surfaces of $BaTiO_3$ doped with 0·75 at% Co^{2+} [(a)–(c)] and 0·75 at% La^{3+} [(d)–(f)]. The samples were heated at 1300°C for (a) 2 h; (b), (d) 4 h; (c), (e) 8 h; and (f) 16 h.

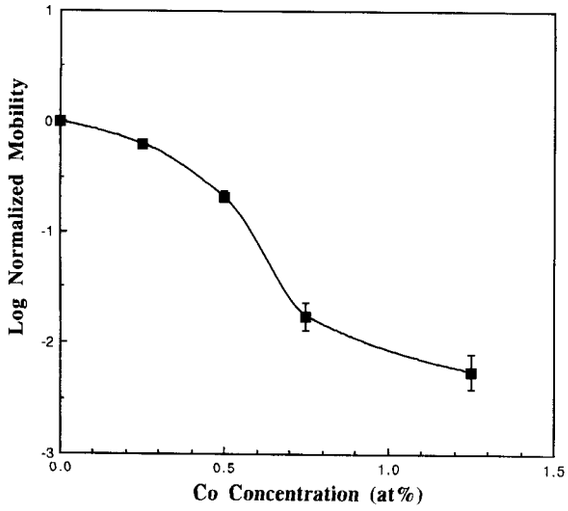

Fig. 8. Grain boundary mobility of Co-doped $BaTiO_3$, normalized to that of undoped $BaTiO_3$, as a function of Co^{2+} concentration.

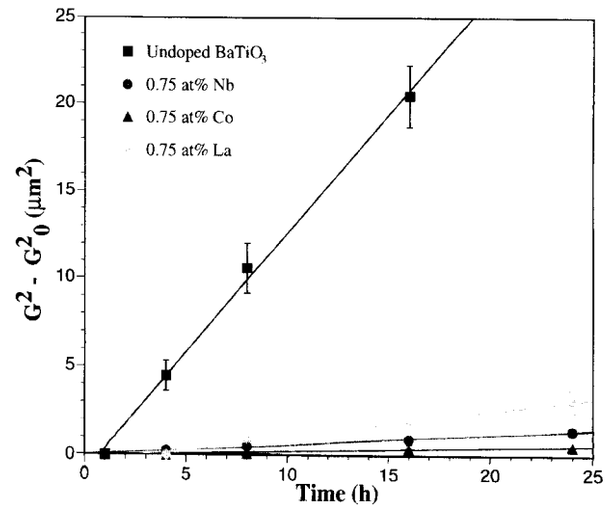

Fig. 9. Grain growth kinetics at 1300°C for undoped $BaTiO_3$ and $BaTiO_3$ doped with 0·75 at% Nb^{5+}, Co^{2+} and La^{3+}.

$$4BaO + 2Nb_2O_5 + BaTiO_3 \Rightarrow 5Ba_{Ba}{}^{X} + 4Nb_{Ti}{}^{\cdot} + 15O_O{}^{X} + TiO_2 + V_{Ti}{}^{''''} \quad (5)$$

In the grain boundary model of Chiang and Takagi[21] discussed earlier, electrons and titanium vacancies are expected to accumulate in the negative space charge. Below the doping threshold, the mechanism for the small enhancement of M_b with increasing Nb^{5+} concentration is not clear. Above the threshold, the accumulation of Ti vacancies in the space charge may be associated with a depletion of oxygen vacancies. Because of their relatively large size, the diffusivity of oxygen ions across the grain boundary is expected to be slow. The low diffusivity of oxygen ions across the grain boundary provides a possible mechanism for the significant reduction in M_b.

In earlier work,[4] the use of double dopants consisting of a donor (Ta^{5+}) and an acceptor (Co^{2+}) indicated that charge compensation has an important effect on M_b. Similar results[28] were also found for co-doping with Nb^{5+} and Co^{2+}. As long as the Nb^{5+} concentration was approximately twice that of Co^{2+} concentration, the boundary mobility was approximately equal to that of the undoped $BaTiO_3$. If, as discussed above, the single dopants Nb^{5+} and Co^{2+} influence M_b by different mechanisms, then an important question is concerned with why charge compensation should have the significant observed effect. A possible explanation for the effect of the double dopants on M_b is that segregation of the acceptor cations and the cation vacancies [given in eqn (5)] does not occur. This may be caused by a reduction of the grain boundary potential to a value considerably smaller than that for $BaTiO_3$ doped with single dopants. At other concentrations, the excess of donor or acceptor cations (relative to the charge-compensated values) leads to effects similar to those produced by the single dopants at the equivalent concentration.[28]

5 Conclusions

In $BaTiO_3$, a major role of donor cations (Nb^{5+} for Ti^{4+} and La^{3+} for Ba^{2+}) and acceptor cations (Co^{2+} for Ti^{4+}) is their ability to influence the boundary mobility. For the acceptor dopant, the boundary mobility decreases monotonically with increasing Co^{2+} concentration. In the case of Nb-doped $BaTiO_3$, the boundary mobility increases slowly with the cation concentration but then decreases significantly above a doping threshold of 0·3–0·5 at%. For the acceptor dopant and the donor dopant above the doping threshold, the reduction in the boundary mobility can be rationalized in terms of the segregation of defects (acceptor solutes or ionic vacancies) at the grain boundaries by a space charge mechanism.

References

1. Coble, R. L., Sintering of crystalline solids: II. experimental test of diffusion models in porous compacts. *J. Appl. Phys.*, 1961, **32**(7), 793–799.
2. Brook, R. J., Fabrication principles for the production of ceramics with superior mechanical properties. *Proc. Brit. Ceram. Soc.*, 1982, **32**, 7–24.
3. Bennison, S. J. and Harmer, M. P., A history of the role of MgO in the sintering of α-Al_2O_3. In *Ceramic Transactions*, Vol. 7, ed. C. A. Handwerker, J. E. Blendell and W. A. Kaysser. American Ceramic Society, Westerville, OH, 1990, pp. 13–49.
4. Brook, R. J., Tuan, W. H. and Xue, L. A., Critical issues and future directions in sintering science. In *Ceramic Transactions*, Vol.1B, ed. G. L. Messing, E. R. Fuller and H. Hausner. American Ceramic Society, Columbus, OH, 1988, pp. 811–823.
5. Xue, L. A., Chen, Y. and Brook, R. J., The effect of lanthanide contraction on grain growth in lanthanide-doped $BaTiO_3$. *J. Mater. Sci. Lett.*, 1988, **7**, 1163–1165.
6. Hwang, S.-L. and Chen, I-W., Grain size control of tetragonal zirconia polycrystals using the space charge concept. *J. Am. Ceram. Soc.*, 1990, **73** (11), 3269–3277.
7. Lin, P., Chen, I-W., Penner-Hahn, J. E. and Tien, T. Y., X-ray adsorption studies of ceria with trivalent dopants. *J. Am. Ceram. Soc.*, 1991, **74**(5), 958–967.
8. Chen, P.-L. and Chen, I-W., Role of defect interaction in boundary mobility and cation diffusivity of CeO_2. *J. Am. Ceram. Soc.*, 1994, **77**(9), 2289–2297.
9. Rahaman, M. N. and Zhou, Y. C., Effect of solid solution additives on the sintering of ultra-fine CeO_2 powders. *J. Europ. Ceram. Soc.*, 1995, **15**, 939–950.
10. Brook, R. J., Frontiers of sinterability. In *Ceramic Transactions*, Vol. 7, ed. C. A. Handwerker, J. E. Blendell and W. A. Kaysser. American Ceramic Society, Westerville, OH, 1990, pp. 3–12.
11. Berry, K. A. and Harmer, M. P., Effect of MgO solute on microstructure development in Al_2O_3. *J. Am. Ceram. Soc.*, 1986, **69**(2), 143–149.
12. Kinoshita, K. and Yamaji, A., Grain size effects on dielectric properties in barium titanate ceramics. *J. Appl. Phys.*, 1976, **47**(1), 371–373.
13. Arlt, G., Hennings, D. and DeWith, G., Dielectric properties of fine-grained barium titanate. *J. Appl. Phys.*, 1985, **58**(4), 1619–1625.
14. Brook, R. J., Controlled grain growth. In *Treatise on Materials Science and Technology*, Vol. 9, ed. F. F. Y. Wang. Academic Press, New York, NY, 1976, pp. 331–364.
15. Chan, H. M., Harmer, M. P. and Smyth, D. M., Compensating defects in highly donor-doped $BaTiO_3$. *J. Am. Ceram. Soc.*, 1986, **69**(6), 507–510.
16. Jonker, G. H. and Havinga, E. E., The influence of foreign ions on the crystal lattice of barium titanate. *Mater. Res. Bull.*, 1982, **17**(3), 345–350.
17. Seuter, A. M. J. H., Defect chemistry and electrical transport properties of barium titanate. *Philips Res. Repts. Suppl.*, 1974, **3**, 1–84.
18. Nowotny, J. and Rekas, M., Defect chemistry of $BaTiO_3$. *Solid State Ionics*, 1991, **49**(12), 135–154.
19. Chan, N.-H. and Smyth, D. H., Defect chemistry of donor-doped $BaTiO_3$. *J. Am. Ceram. Soc.*, 1984, **67**(4), 285–288.

20. Chan, N.-H., Sharma, R. K. and Smyth, D. M., Non-stoichiometry in acceptor-doped $BaTiO_3$. *J. Am. Ceram. Soc.*, 1986, **65**(3), 167–170.
21. Chiang, Y.-M. and Takagi, T., Grain boundary chemistry of barium titanate and strontium titanate: I. high temperature equilibrium space charge. *J. Am. Ceram. Soc.*, 1990, **73**(11), 3278–3285.
22. Sharma, R. K., Chan, H. M. and Smyth, D. M., Solubility of TiO_2 in $BaTiO_3$. *J. Am. Ceram. Soc.*, 1981, **64**(8), 448–451.
23. Hu, Y. H., Harmer, M. P. and Smyth, D. M., Solubility of BaO in $BaTiO_3$. *J. Am. Ceram. Soc.*, 1985, **68**(7), 372–376.
24. Kahn, M., Preparation of small-grained and large-grained ceramics from Nb-doped $BaTiO_3$. *J. Am. Ceram. Soc.*, 1971, **54**(9), 452–454.
25. Mendelson, M. I., Average grain size in polycrystalline ceramics. *J. Am. Ceram. Soc.*, 1969, **52**(8), 443–446.
26. Wurst, J. C. and Nelson, J. A., Lineal intercept technique for measuring grain size in two-phase polycrystalline ceramics. *J. Am. Ceram. Soc.*, 1972, **55**(2), 109.
27. Cahn, J. W., The impurity-drag effect in grain boundary motion. *Acta Metall.*, 1962, **10**(9), 789–798.
28. Manalert, R., Dopants and the sintering of fine-grained barium titanate powder. Ph.D. thesis, University of Missouri-Rolla, Rolla, Missouri, USA, 1996.